Wasit Journal of Engineering Sciences

Journal homepage: https://ejuow.uowasit.edu.iq

Influence of fin thickness variation on the thermal performance of metallic foam heat sink laminar condition

Marwa Alaa Muhsen [1], Abbas J. Jubear A. Al-Ameri [1], Hussein R.al-Bugharbee[1]

Affiliations
[1]Department of Mechanical Engineering,
Wasit University,
Wasit, Iraq.

Correspondence
Abbas J.Jubear
abbasaljassani@uowasit.edu.iq

Received
25-September-2022
Revised
12-November-2022
Accepted
5-January-2023

Doi: 10.31185/ejuow.Vol11.Iss1.383

Abstract

In recent years, open-pore metallic foams have been employed in a wide variety of applications owing to the essential qualities that they possess. In the present study, the thermal performance of a finned heat sink made from open-cell copper foam was investigated numerically under laminar forced conditions. The influence of fin thickness, air velocity, and heat fluxes on the average heat sink base temperature to ambient temperature difference, the Nusselt number, and pressure drop were investigated. Fin thickness was generally taken as 2, 5, 7, and 10 mm. Heat fluxes were taken from (600 to 3000) $W/m^{2,}$ while the air velocity was taken from 0.04 to 0.16 m/s. The findings of laminar flow indicate that straight fins with a thickness of 10 mm minimize the temperature difference between the heat sink's base and the surrounding air the most, followed by fins with thicknesses of 7 mm, 5 mm, and 2 mm. At 3000 W/m^2, a change in velocity from 0.04 to 0.16 m/s increases the average base temperature difference (i.e. (T_{base}-T_{amb})) by 118.9% for a heat sink with 10 mm straight fins. . At a heat flow of 600W/m^2, the Nusselt number grew by 72.6%, 60.7%, and 45.7% when fin thickness was raised from 2 mm to 10 mm, 2 mm to 7 mm, and 2 mm to 5 mm, respectively. The results also demonstrate that the pressure drop rises with increasing fin thickness.

Keywords: Open-cell, straight fins, metallic foam, heat sink,laminar flow.

الخلاصة: في السنوات الأخيرة ، تم استخدام المعادن الرغاوية ذات المسام المفتوحة في مجموعة واسعة من التطبيقات بسبب الصفات الأساسية التي تمتلكها. في هذه الدراسة ، تم التحقيق في الأداء الحراري لمشتت الحرارة ذو الزعانف المصنوع من النحاس الرغوي ذات الخلية المفتوحة عدديا في ظل ظروف ذات جريان قسرية رقائقية. تم التحقيق في تأثير سمك الزعنفة وسرعة الهواء وتدفقات الحرارة على متوسط درجة حرارة قاعدة المشتت الحراري نسبة الى درجة حرارة المحيط ورقم نسلت وانخفاض الضغط. تم أخذ سمك الزعنفة بشكل عام على أنه ٢ و ٥ و ٧ و ١٠ مم. تم أخذ تدفقات الحرارة من (٦٠٠ إلى ٣٠٠٠) واط/م ٢ ، بينما تم أخذ سرعة الهواء من ٠,٠٤ إلى ٠,١٦ م/ث. تشير نتائج التدفق الصفحي إلى أن الزعانف المستقيمة بسماكة ١٠ مم تقلل من فرق درجة الحرارة بين قاعدة المشتت الحراري والهواء المحيط أكثر من غيرها ، تليها الزعانف بسماكة ٧ مم و ٥ مم و ٢ مم. عند ٣٠٠٠ واط/م ٢ ، يؤدي التغير في السرعة من ٠,٠٤ إلى ٠,١٦ م/ث إلى زيادة متوسط فرق درجة الحرارة بين قاعدة البالوعة الحرارية والهواء المحيط بنسبة ١١٨,٩ ٪ لمشتت الحرارة مع زعانف مستقيمة ١٠ ملم. . عند تدفق حرارة ٦٠٠ واط / م ٢ ، زاد عدد نسلت بنسبة ٧٢,٦ ٪ و ٦٠,٧ ٪ و ٤٥,٧ ٪ عندما تم زيادة سمك الزعنفة من ٢ مم إلى ١٠ مم و ٢ مم إلى ٧ مم و ٢ مم إلى ٥ مم على التوالي. تظهر النتائج أيضا أن انخفاض الضغط يرتفع مع زيادة سمك الزعنفة.

1. INTRODUCTION

In recent years, open-pore metallic foams have been employed in a wide variety of applications owing to the essential qualities that they possess. These properties include high permeability, low weight compared to size, and efficient thermal performance. Foam metals have been widely used as heat sinks to cool hot components for various applications, especially electronic devices[1]–[3]. Due to the importance of foam metals in practical applications, researchers have dealt with this type of metal extensively in their scientific research, significantly as a heat sink to cool the various components of the devices. Research into ways to improve heat transfer in heat sinks has gained much attention in recent years to meet the increasing demands for improved efficiency.

The performance of slot-jet impingement cooling numerically with six various forms of aluminum foam heat sinks connected to a horizontally heated surface was investigated in [4] study. The findings demonstrate that all these aluminum foam heat sinks can be utilized to improve the cooling process. When comparing jet cooling with and without a heat sink, it is observed that the average Nusselt number can be enhanced by more than 95% by adding the metal foam heat sink. Another study using finned heat sink was presented in [5] work. In that study, the authors have investigated the sintered metal among the regular finned heat sink, and a metal foam heat sink for power module cooling was designed. The results showed that the heat transfer coefficient of the metal foam heat sink is 3.6 times that of the finned heat sink of the equivalent geometric parameter. At the same drop pressure, the air velocity of the metal foam heat sink is lower than that of the finned heat sink. As a result, the air velocity in the foam radiator is lower than that in the finned radiator. Under the same fan power, the gain factor of the four finned metal foam radiators is about 20 times higher than that of the ribbed radiators of the same conditions. Local thermal non-equilibrium (LTNE) and local thermal equilibrium models have also be utilized in the analysis of metallic foam heat sink by the researchers as shown in [6] study. The results showed that the interstitial convective thermal resistance between the solid and fluid phases was much reduced. In addition, the LTE model can effectively take the LTNE model's role for thermal modeling under these circumstances. As a result, this metal foam heat sink has doubled the overall thermal performance of the non-porous heat sink compared to the whole area of the non-porous metal foam heat sink surface area.

[7] studied the fluid flow and heat transfer performance of an aluminum foam heat sink with pin fins (AFPF heat sink). Pore density enhances heat transfer performance in AFPF and AF heat sinks. Compared to the AF heat sink, the AFPF heat sink improves the average Nusselt number by 63.5–68.1%, while the inferred flow resistance increases by 49.2–88.1%. Furthermore, under the same pumping conditions, the AFPF heat sink performs thermally 1.5 times better than the AF heat sink.

[8] proposed a metal foam heat sink with pin fins (MFPF heat sink) to enhance the cooling performance of high-powered electronics with nonuniform heat flow. The increased flow distribution and overall effective thermal conductivity of the MFPF heat sink considerably improve heat transfer performance (ETC). The MFPF heat sink has also been shown to increase the homogeneity of the bottom wall temperature. For MFPF heat sinks, pore density has less impact on performance than porosity, which has more.

Forced air cooling using an open-cell aluminum foam heat sink was suggested by [9]. The battery module is made up of nine aluminum foam heat sinks and eight pouch cells. When compared to a pure air-cooled system, the metal foam may greatly limit battery temperature rise, but it will generate large flow resistance and pressure loss. As a

result, the average surface temperature of batteries drops, but the temperature differential rises when the porosity of aluminum foam is reduced.

[10] studied heat transfer in these materials to better understand and exploit open-cell metal foams in engineering applications. In this research, five 3D models of copper foam were made, varying in porosity (PPI) from 0.82 to 0.90. (10, 20, and 40) Compared to PPI., the findings showed that the pressure drop and heat transfer coefficient were more sensitive to porosity. However, its specific surface area drastically impacted the metal foam's volumetric heat transfer performance. Also, since the metal foam's closed pores acted as obstacles, the pressure drop, heat transfer characteristics, and CHTP were all significantly altered.

In order to better understand how heat sinks (HS) with diverse designs operate in forced convection, [11] used computational fluid dynamics simulations to examine the effect of changing geometric and boundary characteristics. The frontal area of the device increased the pressure drop by at least 38%, but the temperature was 26% and 56% lower than conventional pins and fins HS, respectively, and 9% and 28% lower than the best pins and best fins of this research, respectively.

To better understand the heat transfer properties of a CPU's triangular cylinder chip and the pin-fin heat sink, [12] performed simulations. The pin fin shape with d = 0.8 and TI = 20% showed the maximum heat transmission compared to the smooth channel. A notable benefit of this research was that it allowed researchers to better understand the impact of various characteristics, such as pressure drop, temperature distribution, and perforation level, on the thermal performance of heat sinks.

Various approaches to disperse the heat created by multiple equipment was presented and investigated in [13] study. These approaches include the use of metal foams with porous fins in an attempt to improve fluid-solid interaction. The efficiency, heat transfer coefficients, performance assessment criteria – incorporating both friction and heat transfer factors – and temperature and stream function contours are all shown in the results section. Among the analyzed situations, the decreasing-aligned pin fin design with the largest Darcy number is the best. The metallic foam heat sink optimization was also investigated in [14] study. Different metal foams connected to a copper plate were used to construct these optimal heat sinks. According to the findings, the strip metal foam attached to the copper plate provides the highest heat transfer effect when the air velocity is 1.33 m/s, and the power consumption ratio is 1:1.6. Using forced convection in metal foam bonded to a copper plate, this heat sink significantly improved the heat transfer performance of a micro-channel heat sink.

The objective of the present study is to investigate the effects of the thickness of the copper foam heat sink for maximization of the heat dissipation rate under the mixed convection mode. The shapes of the copper foams are considered for easy manufacturing, as shown in Figs. 1. Moreover, this study established a numerical simulation model of copper foam heat sink to numerically investigate the detailed flow and heat transfer characteristics.

2. Physical model and mathematical formulation

2.1.Physical model

Figure 1 depicts the heat sinks under investigation. The main form of the heat sink fins consists of straight forms. The overall size of the heat sink is b × w × h = 100 mm × 100 mm × 105 mm. The study has been done to investigate the different thicknesses of the fins (d=2, 5, 7, and 10 mm). The thickness of the base of the heat sink is c=5mm.

The heat sink is installed as a domain in the middle of the box enclosure. To avoid flow reversal during the numerical analysis, this process domain inlet and outlet boundaries were placed far enough from the sink. The domain dimensions are L=500, W=200, and H=200 mm shown in Figure 2.

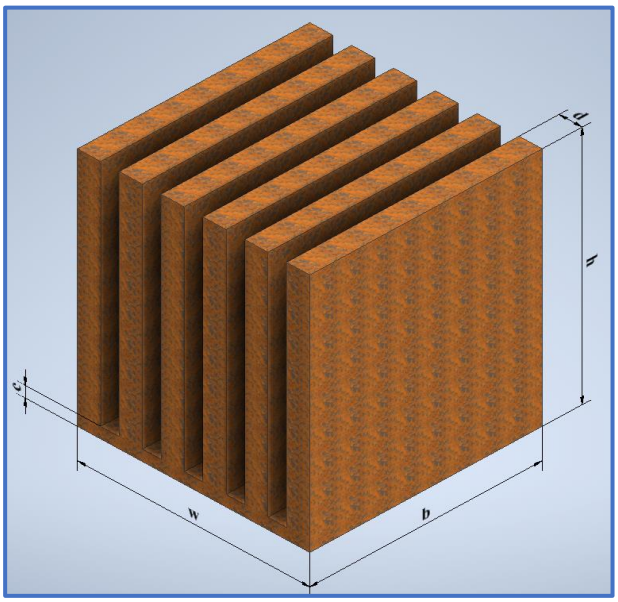

Fig. 1: Heat sink geometry (straight fins)

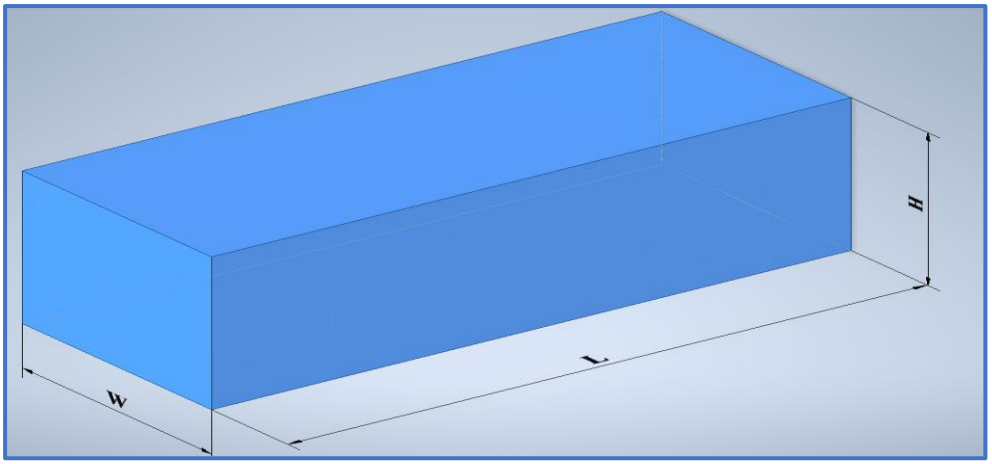

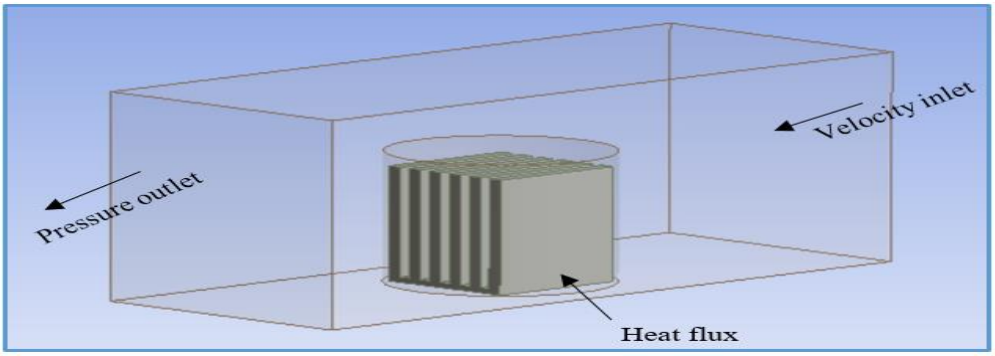

Fig. 2: domain geometry

2.2.Setting Materials

The first step in the creation of a CFD model is the definition of the fluid and material parameters. Various heat sink configurations are constructed of metal foam. The software defines the Copper properties as in table 1.

Table 1: The Materials properties used in the software Ansys fluent.

Fluid	
air	
Density	1.225 kg/m^3
Cp (Specific Heat)	1006.43 J/(kg K)
Thermal Conductivity	0.0242 W/(m K)
Viscosity	1.7894e-05 kg/(m s)
Molecular Weight	28.966 kg/kmol
Thermal Expansion Coefficient	0
Speed of Sound	none
Solid	
copper	
Density	8978 kg/m^3
Cp (Specific Heat)	381 J/(kg K)
Thermal Conductivity	14.290 W/(m K)
aluminum	
Density	2719 kg/m^3
Cp (Specific Heat)	871 J/(kg K)
Thermal Conductivity	202.4 W/(m K)

2.3.Mathematical formulation

2.3.1. Governing equations

The governing equations were linked and solved in a fluent ANSYS software version 22 R1 simulation consisting of momentum equations as well as continuity and energy equations

Continuity Equation

The principles of mass conservation mean that the mass of any closed system remains constant and does not change with time. So, any increase in mass equals the inter-mass flow subtracted from the out-mass flow through the control volumes surface as explained in equations (1) [15] and [16]:

$$\frac{\partial \mathrm{Vx}}{\partial x}+\frac{\partial Vy}{\partial y}+\frac{\partial Vz}{\partial z}=0 \qquad (1)$$

Momentum

The change rate in the momentum of a body is equal to the net force that is acting on it. This is taken from Newton's second law of motion, and it is also named as Navier-Stokes equations, which can be illustrated as the following formulations:

- **Without metal foam (a fluid case)** [15] and [16].

In X-direction

$$V_x\frac{\partial V_x}{\partial x}+V_y\frac{\partial V_x}{\partial y}+V_z\frac{\partial V_x}{\partial z}=-\frac{1}{\rho}\frac{\partial p}{\partial x}+\frac{1}{Re}\left(\frac{\partial^2 V_x}{\partial x^2}+\frac{\partial^2 V_x}{\partial y^2}+\frac{\partial^2 V_x}{\partial z^2}\right) \qquad (2)$$

In Y-direction

$$V_x\frac{\partial V_y}{\partial x}+V_y\frac{\partial V_y}{\partial y}+V_z\frac{\partial V_y}{\partial z}=-g-\frac{1}{\rho}\frac{\partial p}{\partial y}+\frac{1}{Re}\left(\frac{\partial^2 V_y}{\partial x^2}+\frac{\partial^2 V_y}{\partial y^2}+\frac{\partial^2 V_y}{\partial z^2}\right) \qquad (3)$$

In Z-direction

$$V_x\frac{\partial V_z}{\partial x}+V_y\frac{\partial V_z}{\partial y}+V_z\frac{\partial V_z}{\partial z}=-\frac{1}{\rho}\frac{\partial p}{\partial z}+\frac{1}{Re}\left(\frac{\partial^2 V_z}{\partial x^2}+\frac{\partial^2 V_z}{\partial y^2}+\frac{\partial^2 V_z}{\partial z^2}\right) \qquad (4)$$

- **With a metal foam**

In X-direction

$$\frac{1}{\varepsilon^2}\left(V_x\frac{\partial V_x}{\partial x}+V_y\frac{\partial V_x}{\partial y}+V_z\frac{\partial V_x}{\partial z}\right)=-\frac{\partial p}{\partial x}+\frac{1}{\varepsilon\, Re}\left(\frac{\partial^2 V_x}{\partial x^2}+\frac{\partial^2 V_x}{\partial y^2}+\frac{\partial^2 V_x}{\partial z^2}\right)-\frac{1}{Da\, Re}V_x-\frac{F}{\sqrt{Da}}V_x\left|\vec{V}\right| \qquad (5)$$

In Y-direction

$$\frac{1}{\varepsilon^2}\left(V_x\frac{\partial V_y}{\partial x}+V_y\frac{\partial V_y}{\partial y}+V_z\frac{\partial V_y}{\partial z}\right)=-\frac{\partial p}{\partial y}+\frac{1}{\varepsilon\, Re}\left(\frac{\partial^2 V_y}{\partial x^2}+\frac{\partial^2 V_y}{\partial y^2}+\frac{\partial^2 V_y}{\partial z^2}\right)-\frac{1}{Da\, Re}V_y-\frac{F}{\sqrt{Da}}V_y\left|\vec{V}\right| \qquad (6)$$

In Z-direction

$$\frac{1}{\varepsilon^2}\left(V_x\frac{\partial V_z}{\partial x}+V_y\frac{\partial V_z}{\partial y}+V_z\frac{\partial V_z}{\partial z}\right)=-\frac{\partial p}{\partial z}+\frac{1}{\varepsilon\, Re}\left(\frac{\partial^2 V_z}{\partial x^2}+\frac{\partial^2 V_z}{\partial y^2}+\frac{\partial^2 V_z}{\partial z^2}\right)-\frac{1}{Da\, Re}V_z-\frac{F}{\sqrt{Da}}V_z\left|\vec{V}\right| \qquad (7)$$

Energy equations

Energy equation of the fluid in the porous medium (LTNE)

$$\left(V_x\frac{\partial \mathrm{T}_f}{\partial x}+V_y\frac{\partial \mathrm{T}_f}{\partial y}+V_z\frac{\partial \mathrm{T}_f}{\partial z}\right)=\frac{(1+k_f)}{\mathrm{Pr}\,Re}\left(\frac{\partial^2 T_f}{\partial y^2}+\frac{\partial^2 T_f}{\partial z^2}\right)+\frac{h_{sf}a_{sf}}{K_{sf}\,\mathrm{Pr}\,Re}\left(T_s-T_f\right) \qquad (8)$$

Energy equation of the solid matrix (LTNE):

$$0=\frac{\partial^2 T_s}{\partial y^2}+\frac{\partial^2 T_s}{\partial z^2}+\frac{h_{sf}a_{sf}}{K_{se}}\left(T_f-T_s\right) \qquad (9)$$

2.4.Grid independent test

An unstructured grid was used in the computational domain, including a hexahedron grid for the heat sink, which was used in this work. This test was carried out at a heat flux of 600 W/m^2.K with an inlet velocity of 0.3 m/sec. To demonstrate the influence of the element numbers changing from 1000003 to 1052874, the heat sink base wall temperatures have been demonstrated in table 2 and Fig. Error! No text of specified style in document.. As it can be observed, the change in the element numbers had no meaningful impact on the change in temperature values throughout the period studied. As a result, in this numerical investigation, element number 1030133 was chosen.

Table 2: Mesh independence test for the heat sink at HF=600 W/m^2.K and V=0.3 m/s

NUMBER OF ELEMENTS	T_{WALL} (K)
1000003	326.564
1012117	326.862
1030133	327.522
1052874	327.983

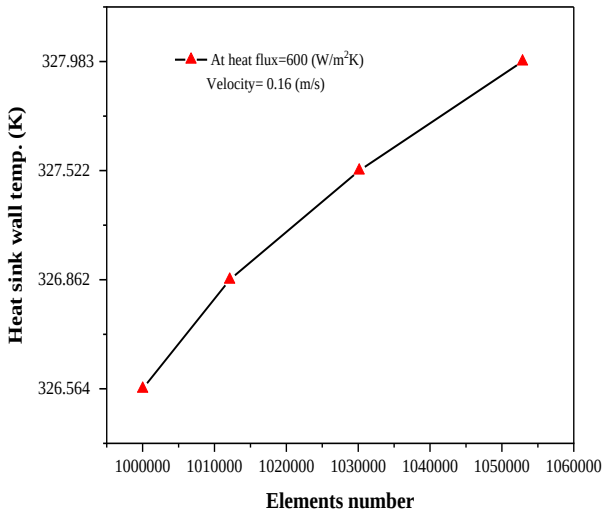

Fig. Error! No text of specified style in document.**:** Mesh independency of the numerical model.

2.5.The verification

To ensure its validity, the CFD results obtained from fluency in this work were compared to the experiments conducted in [18] investigations. The experimental test rig contains a wind channel, a heat supply, a test section, and a data collection device. Acrylic plate with a 5 mm thickness and Aeroflot insulation cover the rectangular wind channel to decrease heat loss. The channels have a width of 0.075 m, a length of 0.8 m, and a height of 0.027 m. The fan is variable speed with an inverter is put at the intake section to regulate the air velocity between 1 and 5 m/s. Pre-air straightening reduces swirling-induced lateral velocity components before the air is introduced into the test section. The heat supply set can control the heat sink base surface temperature. It is made up of a heater powered by electricity and a transformer with a changeable alternating current. The heat sink base is coupled to a 100 W plate heater with a 27-mm width, 75-mm length, and 2-mm thickness. The base surface of the heat sink is kept at 70, 90, and 110 ℃. A Bakelite plate with a 20-mm thickness surrounds a plate heater and the base of a heat sink to keep the heat from escaping into the surrounding air. Fig. 4 compares the experimental work of [18] and the simulation results. The comparison shows that this investigation's predicted standard deviation of heat transfer coefficient obtained from the numerical work and the experimental work of [18] is 2.7%.

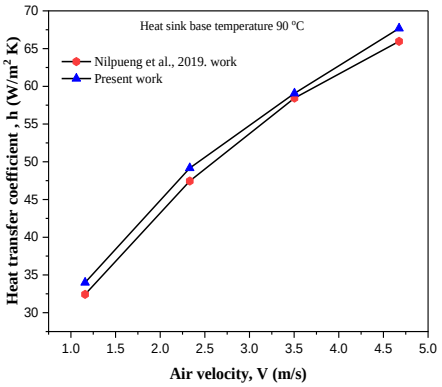

Fig. 4: Comparison of the heat transfer coefficient for the present study with previous experimental study of solid fin heat sink [17]

3. Result and discussion

3.1.Straight fins heat sink performance

The heat sink performance will be interpreted in terms of several varieties such as temperature and velocity vector contours

3.1.1. Temperature and velocity vector contour of the straight fins heat sink

The temperature contour of the straight foam-fin heat sinks with thicknesses of 10,7,5 and 2 mm is shown in Fig. Error! No text of specified style in document. when the heat flux is 600 W/m^2 and the air velocity is 0.16 m/s in a wind channel. It has been demonstrated that temperatures are most significant near the bottom and begin to diminish as the fin's height increases. This means increasing heat transfer by increasing the surface area of the fins; however, when other physical phenomena, such as recirculation zones and velocity variations near the walls, are considered, the surface area may not play a significant role in heat transfer. This phenomenon will be seen in the current study in the following sections when the shape of the fins changes. Furthermore, the figure shows that the temperature is maximum at the heat sink's base and the angles between the fins and the heat sink base. This can be explained by the creation of recirculation zones and the slowing of the flow velocity due to the high friction of air with the fins and the heat sink's base. In addition, it is noted that 10 mm of foam fin thickness provides the highest heat transfer dissipation since the foam fins with the most significant size allow the most considerable amount of air to pass through the pores of the foam and thus absorb the highest amount of heat.

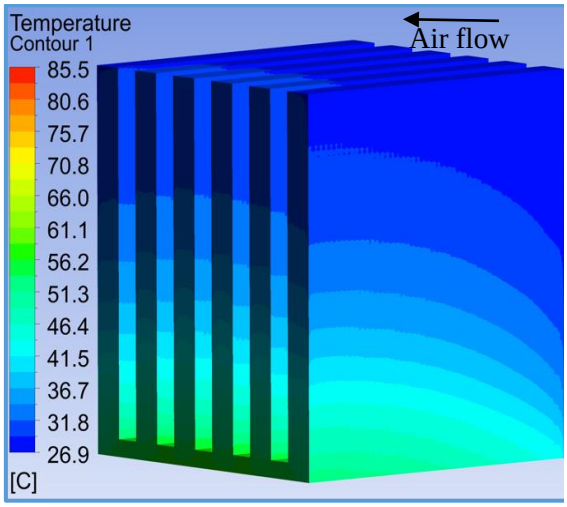

(a)

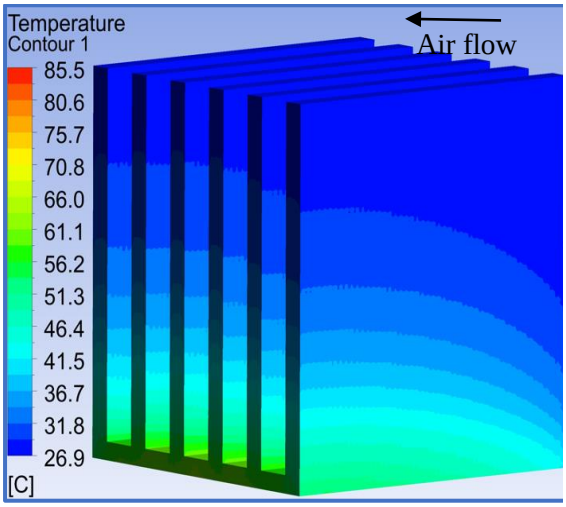

(b)

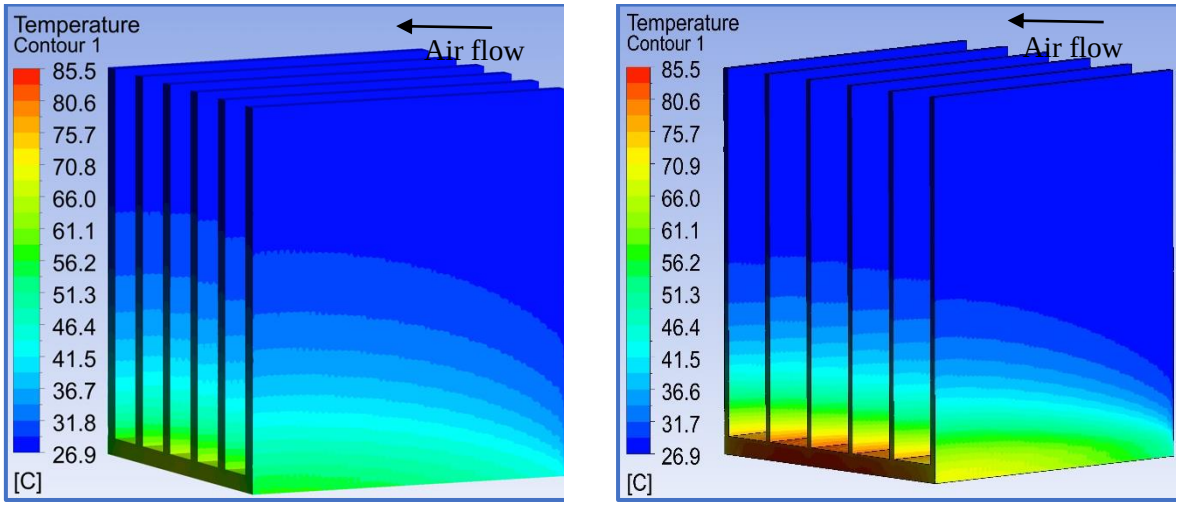

(c) (d)

Fig. Error! No text of specified style in document.**:** the contour of temperature for straight fins, a: 10mm, b: 7mm, c: 5mm, and d: 2mm

Fig. shows the temperature distribution in a plane selected in the center of the base of each heat sink. The outlet air temperature seems to be much warmer than that flowing in. Heat is transferred from the heat sink base and fins to the surrounding air through the air's forced convection. Moreover, the results show that the temperature distribution in the middle of the base with 10 mm fin thicknesses is less than the other heat sink base.

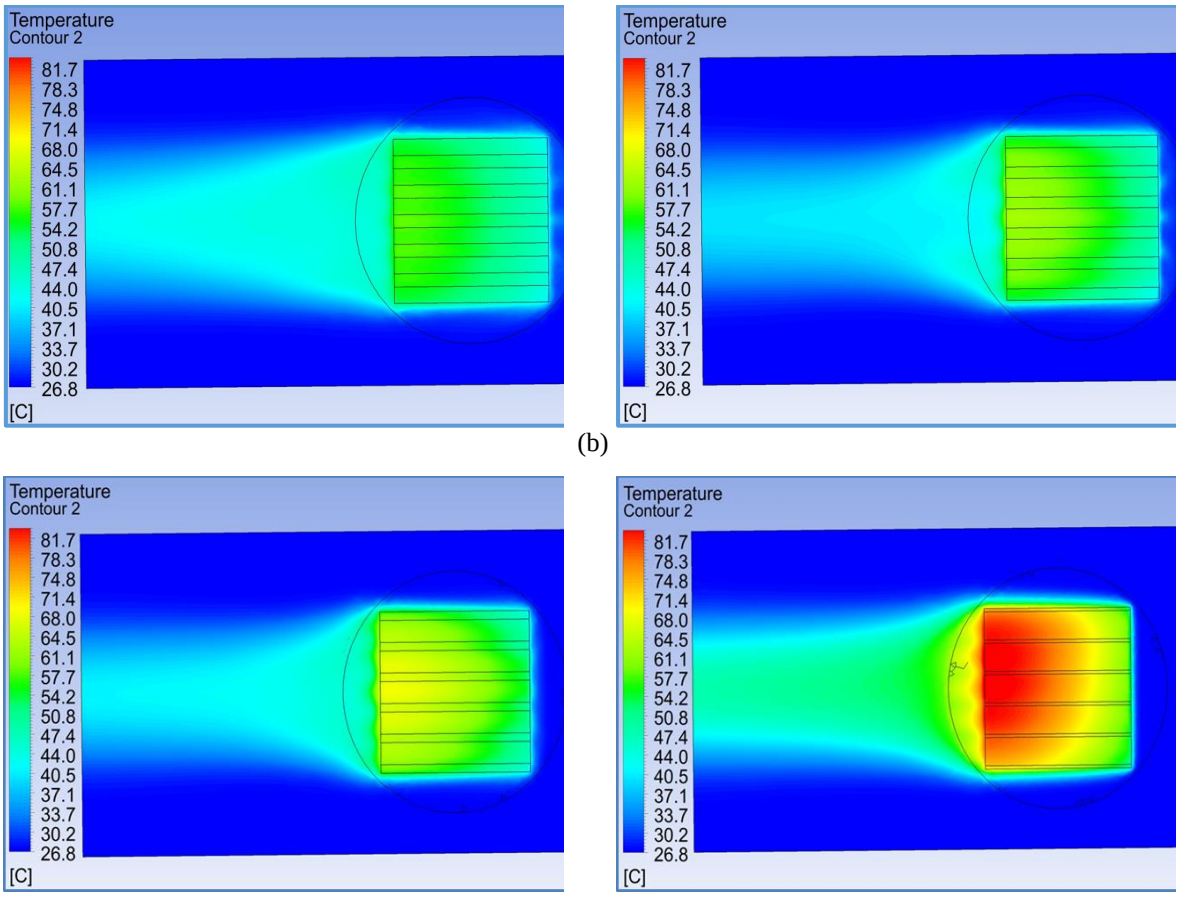

(a) (b)

(c) (d)

Fig. 6: Shows the temperature contour for straight fins, a: 10mm, b: 7mm, c: 5mm, and d: 2mm

Error! Reference source not found. shows the velocity vector contour at a cross-section of 0.025 m from the heat sink base. The velocity of air entering the channel is 0.16 m/s, and the heat flux on the heat sink base is 600 W/m^2.

The numerical simulation was conducted on heat sinks of different fin thicknesses (i.e., 10, 7, 5, and 2 mm). The numerical results illustrated that the flow velocity among the fins of a heat sink with a fin thickness of 10 mm was the highest, followed by heat sinks with fin thicknesses of 7, 5, and 2, respectively. This is since the distance between the heat sink fins is the smallest. Therefore, the airflow velocity between parallel surfaces increases, and the air quantity as the distance decreases. In addition, it is shown that the air passing through the pores of the fins with a thickness of 10 mm is higher than the other thickness of the heat sink fins. Therefore, heat transfer in a heat sink with a thickness of 10 mm is considered higher than in other heat sinks, as shown in the previous section of this study.

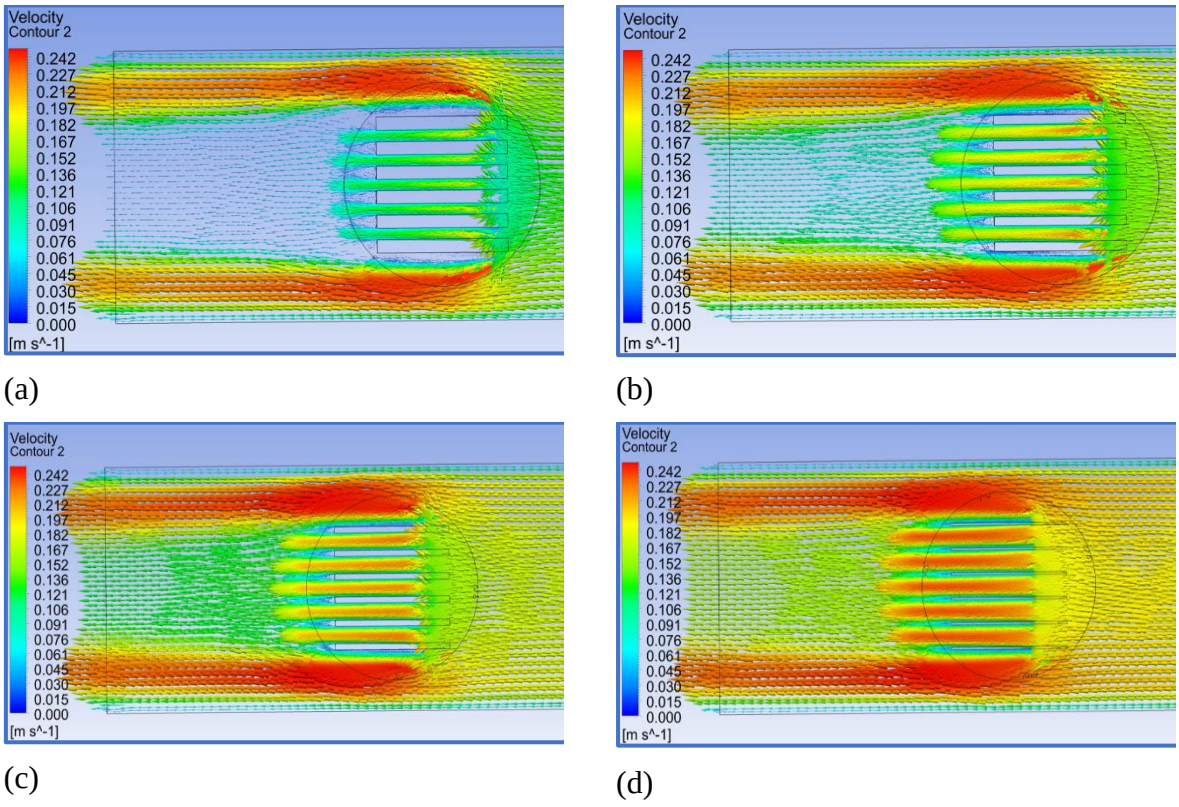

Fig. 7: The vector contour of air for straight foam fin, a: 10mm, b: 7mm, c: 5mm, d: 2mm

3.1.2. Effect of the airflow velocity on straight fins heat sink performance

The influence of airflow velocity on the heat sink base temperature is shown in this section for airflow speeds of 0.04, 0.07, 0.1, 0.13, and 0.16 m/s. Reynolds numbers (ranging from 547 to 2190). Fig. depicts the difference between the average base temperature and the ambient as a function of different heat inputs and airflow velocities. From the results, it is clearly noticed that the average temperature difference increases with the increase of the heat inputs. This is true regardless of the airflow velocity.

It has also been observed that raising the airflow velocities causes the heat sink's base temperature to decrease. This is owing to the increased effectiveness of the heat sink in heat dissipation. Therefore, the heat transfer rate will be reduced due to these changes. It is also noted that the temperature difference between the base of the heat sink and the ambient is the lowest for fins with a thickness of 10 mm, followed by fins 7, 5, and 2 mm, respectively. This is due to the previously mentioned fact that the larger the surface area of the fins, the greater the heat transfer to the ambient. The enhancement of average base temperature difference (i.e. (T_{base}-T_{amb})) is 118.9 % at 3000 W/m^2 when the velocity change from 0.04 to 0.16 m/s for the 10 mm heat sink. Moreover, the enhancement at 600W/m2 is 186% in a similar condition.

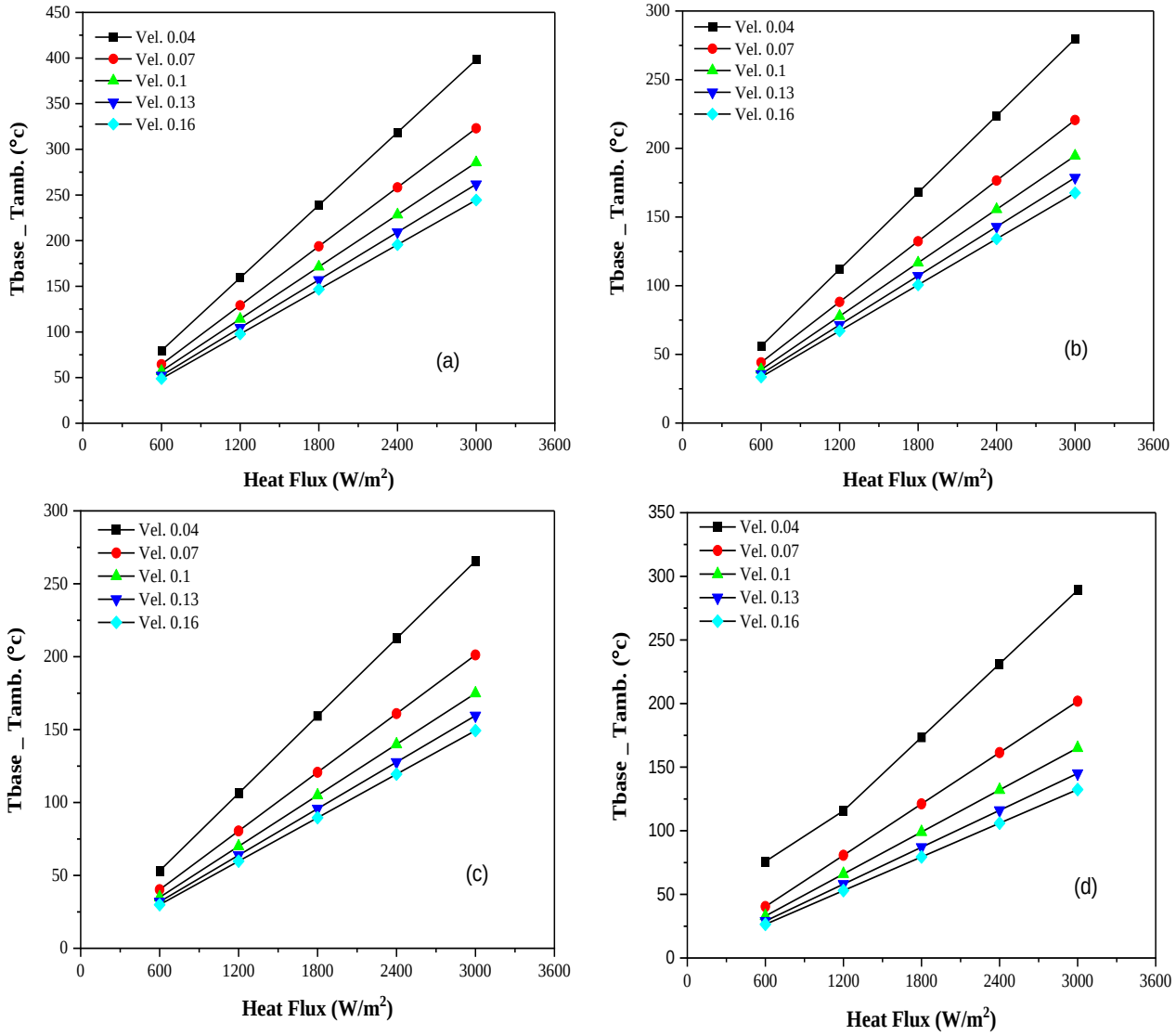

Fig. 8: Effect of the airflow velocity on base to the ambient temperature difference straight foam heat sink, a:2mm, b:5mm, c:7mm, and d:10mm.

3.1.3. Effect of straight fins thicknesses on heat sink performance

Choosing the optimal fin thickness for a given application while considering all relevant economic, operational, cost, weight, and availability aspects are critical to increasing heat transfer and enhancing the heat sink's efficiency. The impact of altering the thickness of fins (2, 5, 7, and 10 mm) on the heat sink's performance is discussed in this section.

The relationship between the temperature change of the heat sink base and the thickness of the fin changes is shown in Fig. . The numerical analysis is performed when the heat flux changes and the flow velocity is fixed at 0.16 m/s.

The results indicate that the temperature of the heat sink's base has increased as the heat flux value on the base of the heat sink has increased. It also is noticed from this figure that the temperature of the heat sink's base decreases as the thickness of the fins increases. As mentioned earlier, the surface area plays a crucial role in changing the temperature base of the heat sink. As the surface area of the fins increases, the heat transfer coefficient rises proportionally. Furthermore, expanding the fin foam's surface area allows the greatest amount of air to enter through the fin's pores, resulting in the greatest amount of heat being absorbed. When the thickness is changed from 2 to 10 mm, there is an increase of 84.59 percent in the average base temperature (T_{base} - T_{amb}) at 3000 W/m^{2,} while a 63.6% enhancement is observed at 600 W/m^2.

The obtained results also showed an improvement of 25.6% and 63.67% when the thickness was increased from 2 to 7 mm at 3000 W/m^2 and 600 W/m^{2,} respectively. In comparison, a slight enhancement is noticed when fins

thickness is changed from 2 to5 mm, where 26.5% and 65.5% are obtained at 3000 W/m^2 and 600 W/m^{2,} respectively

Based on the above, it is clarified that the impact of the fin thickness increment is more significant with higher heat flux.

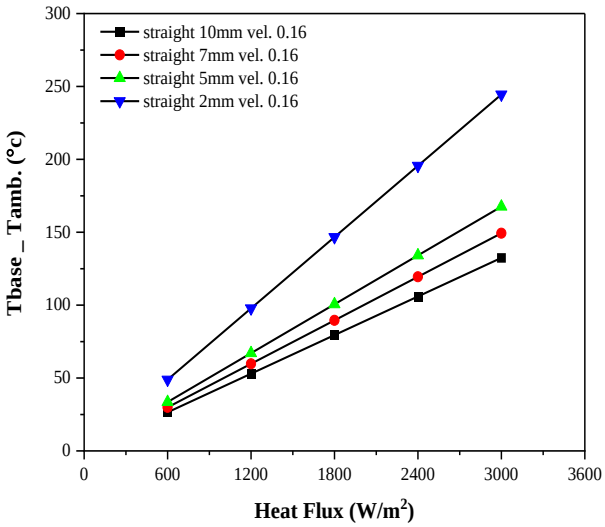

Fig. 9: Effect of straight fins thicknesses on heat sink performance

3.1.4. Effect of the Reynold on Nusselt number

The relation between Nusselt numbers and Reynolds numbers (ranging from 547 to 2190) is shown in Fig. , a constant heat input of 600 W. The rising value of the Reynolds number led to a rise in the Nusselt number. This is because the inertia force impact was more substantial than the viscous force. The Nusselt number appears to increase with the increasing thickness of the fin, which leads to a reduction in the temperature difference. Increased heat transfer coefficients can be achieved by thickening the fins since this will increase the surface area of the heat dissipation. The enhancement of Nusselt number due to heat transfer coefficient was 72.6 %, 60.7%, and 45.8% when fin thickness is increased from 2 to 10 mm, 2 to 7 mm, and 2 to 5 mm, respectively, at a heat flux of 600W/m^2, and with 10 mm fin thickness, the Nusselt number increase was 11.84 % more than with 7 mm thickness compared with the 2 mm, and 26.7% percent more than with 5mm thickness.

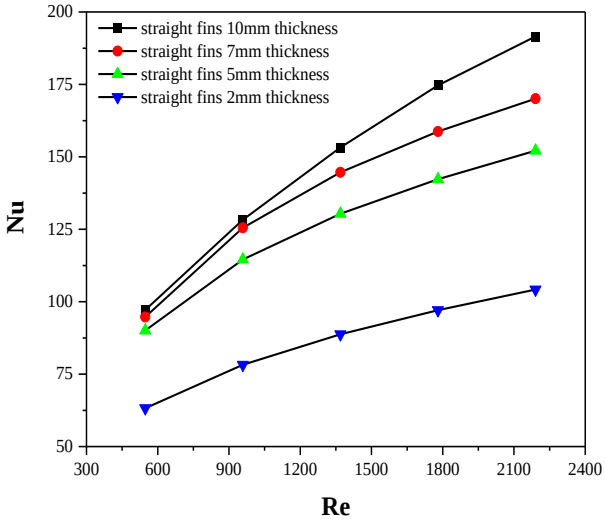

Fig. 10: Effect of Reynolds number on Nusselt number for different thickness fins of the straight heat sink

3.1.5. Effect of the Reynolds number on pressure drop

In this part of the study, the pressure drop was calculated when the thickness of the straight and wavy fins of the heat sink changed from 2 mm to 10 mm. The calculations were also made at different Reynolds numbers, as shown in Fig. . Numerical results indicate that the pressure drop increases as the flow velocity increases. They also indicate that the pressure drop increases as the fin thickness of the heat sink increases. This is because the body's resistance to air increases with the increase of fin thickness.

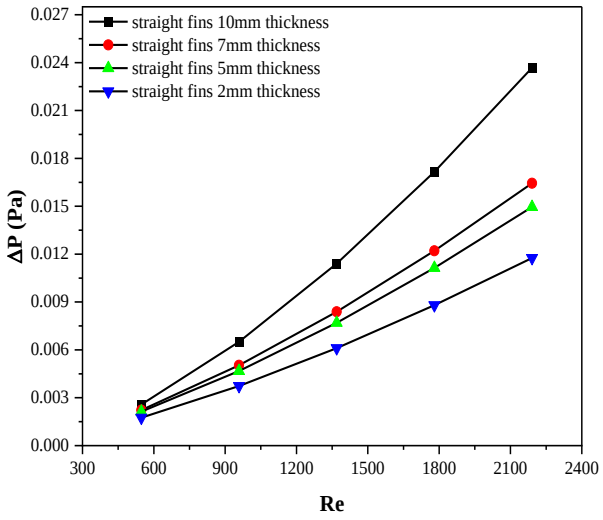

Fig. 11: Effect of the different thicknesses of the straight fins heat sink on pressure drop

3.2.Results of an empirical equation

Table 3 shows the nonlinear regression coefficients and the regression's mean absolute error. The regression shows a very good agreement with only %6.77 of mean absolute error.

$$N_u = -663.1594 + 480.1802 * S^{0.0724} + 51.8201 * Re^{0.2181} + \varepsilon \quad (5)$$

Table (3): Coefficients of nonlinear regression- Laminar

c_0	c_1	c_2	c_3	c_4	**% Mean ABS =** $\frac{1}{n}\sum_{i=1}^{n}\frac{\lvert Nu_{Th}-Nu_{Predicted}\rvert}{Nu_{Th}} * 100$
-663.1594	480.1802	0.0724	51.8201	0.2181	% 6.77

Figure (12) illustrates the theoretical and predicted values of the Nusselt number. The theoretical values are those obtained from the Ansys simulation, while the predicted values are those obtained from the regression model. The comparison shows a perfect agreement for all of the readings.

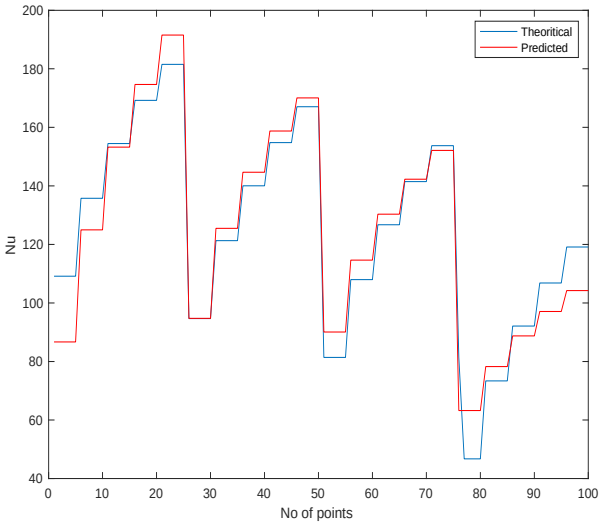

Figure (13) depicted the corelation between the theoretical and predicted Nusselt number values. The comparison shows a very high correlation with R=0.96.

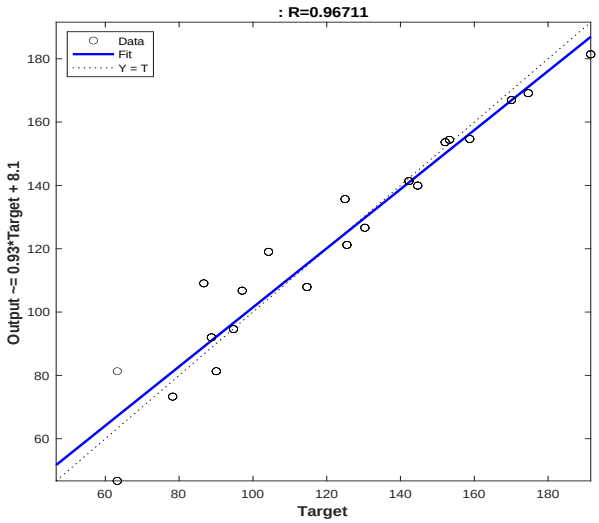

4. Conclusion

It is concluded that both the fin's thickness and air velocity play a significant role in the heat sink's thermal performance. The fin thickness can directly affect the contact area between the fins and the heat sink's base. And on the exact moment, the fin thickness affects the spacing among fins; when the fin thickness increases, the fin spacing decreases.

The air velocity also affects the heat dissipation in a proportional relationship. Therefore, the following finding is concluded:

- The straight fins with a thickness of 10 mm significantly reduce the temperature differential between the heat sink's base and the surrounding air, followed by fins of 7 mm, 5 mm, and 2 mm.

- For a 10 mm straight fins heat sink, a change in velocity from 0.04 to 0.16 m/s results in an increase in average base temperature differential (i.e. (Tbase-Tamb)) of 118.9% at 3000 W/m^2. Additionally, the improvement at 600W/m^2 is 186% under the same conditions.

- The average base temperature (Tbase-Tamb) rises by 84.59% when the thickness is increased from 2 to 10 mm at 3000 W/m^2 and by 63.66% when the heat input is reduced to 600 W/m^2.

- with a thickness increase from 2 to 7 mm, yielding a 25.6% and 63.67 % improvement at 3000 W/m^2 and 600 W/m^2, respectively.

• Increasing the fins' thickness from 2 to 5 mm yields 26.5% at 3000 W/m^2 and 65.5% at 600 W/m^2, respectively.

• Nusselt number improvement due to heat transfer coefficient was 72.6 %, 60.7 %, and 45.7 % when fin thickness was increased from 2 mm to 10 mm, 2 mm to 7 mm, and 2 mm to 5 mm, respectively, at a heat flux of 600 W/ m^2.

• The pressure drop increases as the flow velocity increase for all the shapes. They also indicate that the pressure drop increases as the fin thickness of the heat sink increases.

REFERENCES

[1] A. Alhusseny, Q. Al-Aabidy, N. Al-Zurfi, A. Nasser, and M. Aljanabi, "Cooling of high-performance electronic equipment using graphite foam heat sinks," *Appl. Therm. Eng.*, vol. 191, p. 116844, 2021, doi: https://doi.org/10.1016/j.applthermaleng.2021.116844.

[2] Y. Li, L. Gong, M. Xu, and Y. Joshi, "Enhancing the performance of aluminum foam heat sinks through integrated pin fins," *Int. J. Heat Mass Transf.*, vol. 151, p. 119376, 2020, doi: https://doi.org/10.1016/j.ijheatmasstransfer.2020.119376.

[3] P. Samudre and S. V. Kailas, "Thermal performance enhancement in open-pore metal foam and foam-fin heat sinks for electronics cooling," *Appl. Therm. Eng.*, vol. 205, p. 117885, 2022, doi: https://doi.org/10.1016/j.applthermaleng.2021.117885.

[4] Y. Li, L. Gong, M. Xu, and Y. Joshi, "Hydraulic and thermal performances of metal foam and pin fin hybrid heat sink," *Appl. Therm. Eng.*, vol. 166, p. 114665, 2020, doi: https://doi.org/10.1016/j.applthermaleng.2019.114665.

[5] N. H. Saeid, N. Hasan, and M. H. B. H. M. Ali, "Effect of the metallic foam heat sink shape on the mixed convection jet impingement cooling of a horizontal surface," *J. Porous Media*, vol. 21, no. 4, pp. 295–309, 2018, doi: 10.1615/JPorMedia.v21.i4.10.

[6] G. H. Hao and Y. P. Zhang, "Thermal Performance Simulation of the Metal Foam Heat Sink," in *Solid State Phenomena*, 2019, vol. 298, pp. 208–213.

[7] Y. Li, L. Gong, H. Lu, D. Zhang, and B. Ding, "Thermal modeling and analysis of metal foam heat sink with thermal equilibrium and non-equilibrium models," *C. - Comput. Model. Eng. Sci.*, vol. 123, no. 2, pp. 895–912, 2020, doi: 10.32604/cmes.2020.09009.

[8] Y. Li, L. Gong, M. Xu, and Y. Joshi, "Thermal Performance of Metal Foam Heat Sink With Pin Fins for Nonuniform Heat Flux Electronics Cooling," *J. Electron. Packag.*, vol. 143, no. 1, p. 11006, 2021.

[9] Y. Wang, Y. Yu, Z. Jing, C. Wang, G. Zhou, and W. Zhao, "Thermal performance of lithium-ion batteries applying forced air cooling with an improved aluminium foam heat sink design," *Int. J. Heat Mass Transf.*, vol. 167, p. 120827, 2021, doi: https://doi.org/10.1016/j.ijheatmasstransfer.2020.120827.

[10] M. Sun *et al.*, "Pore-scale simulation of forced convection heat transfer under turbulent conditions in open-cell metal foam," *Chem. Eng. J.*, vol. 389, p. 124427, 2020, doi: 10.1016/j.cej.2020.124427.

[11] E. C. Silva, Á. M. Sampaio, and A. J. Pontes, "Evaluation of active heat sinks design under forced convection—effect of geometric and boundary parameters," *Materials (Basel).*, vol. 14, no. 8, 2021, doi: 10.3390/ma14082041.

[12] M. W. Alam *et al.*, "CPU heat sink cooling by triangular shape micro-pin-fin: Numerical study," *Int. Commun. Heat Mass Transf.*, vol. 112, p. 104455, 2020, doi: https://doi.org/10.1016/j.icheatmasstransfer.2019.104455.

[13] A. M. Ranjbar, Z. Pouransari, and M. Siavashi, "Improved design of heat sink including porous pin fins with different arrangements: A numerical turbulent flow and heat transfer study," *Appl. Therm. Eng.*, vol. 198, p. 117519, 2021, doi: https://doi.org/10.1016/j.applthermaleng.2021.117519.

[14] Z. Zhong, L. Meng, X. Li, G. Zhang, Y. Xu, and J. Deng, "Enhanced heat transfer performance of optimized micro-channel heat sink via forced convection in cooling metal foam attached on copper plate," *J. Energy Storage*, vol. 30, p. 101501, 2020, doi: https://doi.org/10.1016/j.est.2020.101501.

[15] M. A. Nim and A. H. Hajeej, "Numerical Study of Mixed Convection Heat Transfer Enhancement in a Horizontal Channel by Adding Metal Foam Blocks," vol. 17, no. July, pp. 223–241, 2017.

[16] L. F. Ali, "Natural and Mixed Convection in Square Vented Enclosure Filled with Metal Foam," *J. Eng.*, vol. 21, no. 11, pp. 60–79, 2015.

[17] S. Mahjoob and K. Vafai, "A synthesis of fluid and thermal transport models for metal foam heat exchangers," *Int. J. Heat Mass Transf.*, vol. 51, no. 15–16, pp. 3701–3711, 2008.

[18] K. Nilpueng, H. S. Ahn, D.-W. Jerng, and S. Wongwises, "Heat transfer and flow characteristics of sinusoidal wavy plate fin heat sink with and without crosscut flow control," *Int. J. Heat Mass Transf.*, vol. 137, pp. 565–572, 2019.